Performance Analysis of THz Enabled HetNets in Diverse Building Densities

Muhammad Hassaan[1], Muhammad Bin Azhar[1], Kamran Naveed Syed[1], Syed Ali Hassan[1], Haris Pervaiz[2], Haejoon Jung[3]
[1]School of Electrical Engineering and Computer Science,
National University of Sciences and Technology (NUST), Islamabad, Pakistan
[2]School of Computing & Communications, Lancaster University, UK
[3] Department of Electronic Engineering, Kyung Hee University, Yongin, South Korea
E-mail: {mhassaan.bee18seecs, mazhar.bee18seecs, ksyed.bee18seecs, ali.hassan}@seecs.edu.pk,
h.b.pervaiz@lancaster.ac.uk, haejoonjung@khu.ac.kr

***Abstract*—Beyond 5G networks require low latency, high throughput and high data rates while maintaining appreciable coverage. To achieve this, a wider bandwidth is required. Terahertz (THz) band can provide such large bandwidth, however, it is not as reliable as the sub 6 GHz band due to absorption effects. Hence, we need infrastructure level approaches such as heterogeneous networks (HetNet) that provide backwards compatibility to increase coverage and reliability. In this paper, we consider a HetNet comprised of small base stations at THz and mmWave frequencies, and macro base station at sub-6 GHz frequency at different building densities based on multiple cities around the world. For quality of service (QoS) performance metrics, we take data rate coverage and power efficiency. Different system parameters are varied for six different locations to analyze the effectiveness of the proposed HetNet. Our results show that B5G networks are considerably more effective in environments with low building densities.**

***Index Terms*—Terahertz, mmWave, heterogeneous network, power efficiency**

I. Introduction

As the world moves towards beyond fifth generation (B5G) communications, an ever growing demand arises for ultra reliable low latency communication (URLLC) characterized by higher throughput, higher data rates and lower latencies. The imminent Internet-of-things (IoT) revolution is projected to comprise 25 billion interconnected devices by 2025 [1], which will require ultra high bandwidths and reliability for smart monitoring, control, digital sensing and 360° high-definition video transmission. The incorporation of wireless augmented/virtual reality and immersion technologies in the entertainment industry also imposes quality-of-experience demands that can only be satisfied by high-rate and high reliability low latency communications [2] [3]. Consequently, terabit-per-second (Tbps) links are expected to emerge as key enablers for the next generation of wireless communications. Current millimeter-wave (mmWave) systems, however, fail to meet Tbps data rate demands as the total available bandwidth of mmWave is limited to less than 10GHz. The terahertz (THz) band (0.1-10 THz) with its high bandwidths will, thus, emerge to fulfill the demands of future 6G systems.

THz communication is projected to overcome capacity limits of currently available wireless channels and meet real-time traffic demands for 6G mobile heterogeneous networks (HetNets) of the future. Low-frequency (sub-6 GHz) bands of traditional base stations (BSs) offer limited bandwidth. The deployment of THz and mmWave enabled BSs however, can fulfill high data rate demands. THz comes with its own challenges in the form of high propagation losses and limited communication distance [4]. At frequencies as high as THz, molecular absorption also becomes a major factor. Thus, a compromise has to be reached between higher bandwidth/data rates and high propagation losses. The integration of these technologies in HetNets and their subsequent performance has become a focus of research to meet the ever-increasing demands of ultra-high data rates [5].

In this paper, we present the analysis of THz and mmWave assisted HetNets to maximize power efficiency (bits/joule). For this purpose, we present a multi-tier hybrid HetNets consisting of macro base stations (MBS) operating at sub-6 GHz band with multiple small base stations (SBS) operating at THz and mmWave frequency bands deployed in 6 regions around the world with varying building densities. Instead of the traditional approach to use estimated line of sight (LOS) and non-line of sight (NLOS) probabilities for simulations, we calculate the LOS and NLOS links for each map using real environments. The inclusion of real world building data simulates blockage effects and includes environmental geometry into our analysis to evaluate the performance of the described HetNet if deployed in these regions.

II. System Model

The proposed HetNet consists of 3-tiers: THz and mmWave enabled small BSs and sub-6 GHz macro BSs providing coverage to N users as depicted in Figure 1. All the base stations are assumed to have their independent backhaul capabilities by fiber links. In this paper, we have used actual building locations for 6 different areas around the world, comprising a wide range of building densities. This provides real world blockage effects and environmental geometry for our analysis. Figure 2 shows one such area which represents Google earth view of the NUST campus, while Figure 3 shows actual building locations extracted by MATLAB. The building densities are calculated using Quantum Geographic Information

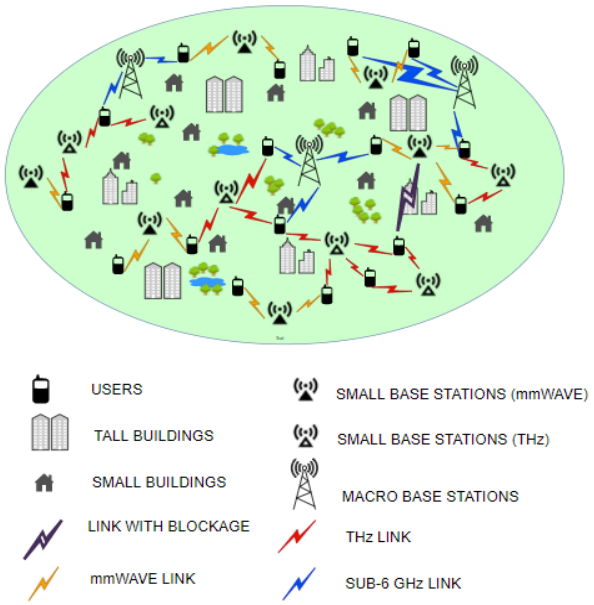

Fig. 1. Graphical representation of the proposed HetNets with multiple MBS, as well as mmWave and THz enabled small base stations.

System (QGIS) software. Some key building statistics along with corresponding areas are provided in Table 1.

TABLE I
TOTAL CAPTURED AREA AND PERCENTAGE BUILDING DENSITY FOR 6 LOCATIONS

Location	Total Area (m^2)	Building area (m^2)
NUST, Islamabad	1609938	5.03 %
Golra, Rawalpindi	1608505	9.11 %
F11, Islamabad	1150352	14.63 %
London	4036264	34.86 %
Manchester	1011248	40.54 %
New York	1331042	53.1 %

Moreover, the number of users and BSs are randomized by two dimensional homogeneous poisson point process (HPPP) with the BS density of each tier: σ_j where $j \in \{$MBS, THz, mmWave$\}$ while the locations of both users and BSs are uniformly distributed.

The users have been considered in both indoor and outdoor regions. BSs may also lie on the building rooftops. If the communication link between the user and BS is blocked by a building, it is considered NLoS, otherwise it is considered to be LoS, with corresponding path loss considerations. For small scale fading between BS and the user, Nakagami fading model is used with fading envelope given by the following probability density function [6]

$$|\nu| \sim f_{|\nu|}(x, \mu_q) \approx \frac{\mu_q^{\mu_q} x^{\mu_q - 1} exp\{-\mu_q x\}}{\gamma(\mu_q)}, \forall x > 0\,, \quad (1)$$

where μ_q is the Nakagami fading parameter and $q \in \{L_m, N_m\}$. L_m and N_m are LoS and NLoS propagation environments respectively and $\gamma(\mu_q)$ is the gamma function.

Fig. 2. Google Earth image of NUST campus

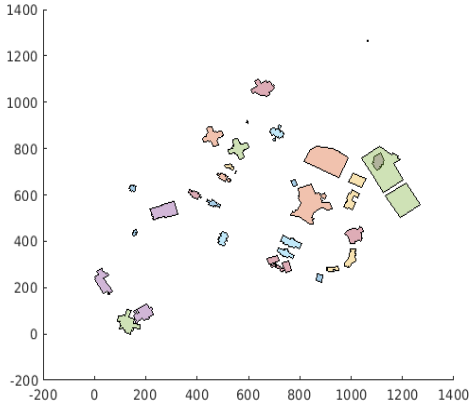

Fig. 3. Recreated buildings of NUST campus in MATLAB

Both μ_{L_m} and μ_{N_m} are positive integers [6] while μ_q for macro base station is considered to be 1 [6]. The path loss model for sub-6 GHz band is given by

$$\mathrm{PL}_{\mathrm{MBS}} = 20\log\left(\frac{4\pi}{\lambda_c^{\mathrm{MBS}}}\right) + 10\alpha\log(d) + \chi\,, \quad (2)$$

where λ_c^{MBS} is the wavelength corresponding to carrier frequency, d is the distance between MBS and the user, α is the path loss exponent and χ defines shadow fading.

The path loss for mmWave link $\mathrm{PL}_{mmWave}(d)$ in dB is given by

$$\mathrm{PL}_{\mathrm{mmWave}} = \begin{cases} \rho + 10\alpha_L \log(d) + \chi_L & \text{if link is LoS} \\ \rho + 10\alpha_N \log(d) + \chi_N & \text{if link is NLoS} \end{cases}, \quad (3)$$

where χ_L and χ_N model the effects of shadow fading as they are the zero mean log normal variables for LoS and NLoS mmWave links, respectively. The fixed path loss, ρ, is given by $\rho = 32.4 + 20\log(f_c)$ where f_c is the carrier frequency. The path loss exponents for LoS and NLoS mmWave links are denoted by α_L and α_N, respectively.

The path loss model similar to [7] for THz small base station can be expressed as

$$\mathrm{PL_{THz}} = \mathrm{PL}(f,d)_{spread} + \mathrm{PL}(f,d)_{absorption}\,, \tag{4}$$

similar to [8], where $\mathrm{PL}(f,d)_{spread}$ is the spreading loss due to the expansion of wave when it travels through the medium and is given as

$$\mathrm{PL}(f,d)_{spread} = 20\log\left(\frac{4\pi f_c d}{c}\right), \tag{5}$$

where f_c is the THz carrier frequency, c is the speed of light and d is the distance between user and small base station.

$\mathrm{PL}(f,d)_{absorption}$ is the attenuation in the EM wave which is caused by molecular absorption and is given by

$$\mathrm{PL}(f,d)_{absorbtion} = \frac{1}{\tau(f,d)} = exp^{k(f)d}\,, \tag{6}$$

where τ is the transmittance of the medium, f_c is THz frequency and $k(f)$ is frequency dependent molecular absorption coefficient [9], which is calculated by using radiative transfer theory and the information provided by the high resolution transmission molecular absorption (HITRAN) database [10].

The received power of a user associated with tier j at a distance d is calculated by

$$\begin{aligned} P_{r,j}[\mathrm{dB}] = P_{t,j} + G(\phi_j) + \mu_j - PL_j : \\ j \in \{MBS, mmWave, THz\}\,, \end{aligned} \tag{7}$$

where μ_j is the Nakagami multi-path fading and $G(\phi_j)$ is the directional antenna gain [11], given by

$$G(\phi_j)[\mathrm{dB}] = \begin{cases} 0 & j \in MBS \\ \frac{Y}{\omega_h \times \omega_v} = \frac{Y}{\omega^2} & j \in \{mmWave,\ THz\} \end{cases}, \tag{8}$$

$$\mu_j[\mathrm{dB}] = \begin{cases} 0 & j \in MBS \\ \mu_q & j \in \{mmWave,\ THz\}, q \in \{LoS, NLoS\} \end{cases}, \tag{9}$$

The received power of a user associated with tier j is given by

$$P_{r,j}[\mathrm{dB}] = P_{t,j} - \mathrm{PL}_j\,, \tag{10}$$

where $P_{r,j}, P_{t,j}$ and PL_j are the received power, transmitted power and path loss for tier j, respectively.

III. Performance Analysis

Due to dense BS deployment, each user receives power from multiple adjacent base stations of all three tiers. In order to associate with a particular base station k the user analyses all the received powers and associates with the one with maximum received power.

$$\mathrm{A}_u = \arg\max_{k,j} P_{r,k,j}\,, \tag{11}$$

The cumulative associativity, A_j, for each tier can be calculated by

$$\mathrm{A}_j = \frac{U_j}{U}\,, \tag{12}$$

where U is the total number of users and U_j is the number of users associated with the tier j. The users associated to any of the tiers will experience interference from other users of the same tier which will affect their data rate. For that we calculate the signal-to-interference plus noise ratio (SINR) received by user u associated with tier j by

$$\mathrm{SINR}_{u,j} = \frac{P_{r,j}}{\Sigma_{i\in\{MBS,\,mmWave\,and\,THz\}} P_i + \sigma^2}\,, \tag{13}$$

where P_i is the cumulative interference from all users associated with the same tier to the user u and σ^2 is the noise power spectral density. For downlink transmission, the achievable data rate for each user in tier j is given by

$$R_{u,j} = \frac{\mathrm{B}_j}{U_j} \times log_2(1 + \mathrm{SINR}_{u,j})\,, \tag{14}$$

where B_j and U_j are the total available bandwidth and total number of users associated in tier j with a particular base station, respectively.

The SINR coverage probability at a given threshold ζ_j is given by

$$P_{conv,j}(\zeta) = \mathbb{P}(\mathrm{SINR}_{u,j} > \zeta_j)\,, \tag{15}$$

Similarly, the rate coverage probability at a given threshold η_j is computed as

$$P_{Rate,j}(\eta_j) = \mathbb{P}(R_{u,j}^{effective} > \eta_j) = \mathbb{P}(\mathrm{SINR}_{u,j} > 2^{\frac{\eta_j \times U_j}{B_j}} - 1)\,, \tag{16}$$

Resultantly, the total SINR coverage probability $P_{coverage}(\zeta)$ and the total rate coverage probability $P_{effective\,rate}(\eta)$ are calculated using total law of probability as

$$P_{\mathrm{SINR}}(\zeta) = \sum_{j\in J} \mathrm{A}_j \times P_{conv,j}(\zeta_j)\,, \tag{17}$$

and

$$P_{effective\,rate}(\eta) = \sum_{j\in J} \mathrm{A}_j \times P_{Rate,j}(\eta_j)\,, \tag{18}$$

where again $j \in \{\mathrm{MBS},\ \mathrm{THz},\ \mathrm{mmWave}\}$, A_j is the association probability of tier j and $P_{conv,j}(\zeta),\ P_{rate,j}(\eta)$ are coverage probabilities of tier j with their threshold, respectively.

Consider the power efficiency of the system given by

$$\kappa = \frac{R}{\lambda_{MBS}.P_{\mathrm{MBS}} + \lambda_{mmWave}.P_{\mathrm{mmWave}} + \lambda_{THz}.P_{\mathrm{THz}}}\,, \tag{19}$$

where R denotes the system sum rate per unit area across all the three tiers. The term in the denominator represents the energy consumption of system on a per unit area basis. Rearranging the terms and isolating λ_{THz} we get,

$$\lambda_{\mathrm{THz}} = \frac{m(R-k)}{\kappa(m.P_{\mathrm{THz}} - P_{\mathrm{mmWave}})}\,, \tag{20}$$

where m and k are given by $\frac{\lambda_{THz}}{\lambda_{mmWave}}$ and $\lambda_{MBS} \times P_{\mathrm{MBS}}$ respectively. Rate coverage probability is calculated for different values of m while maintaining the rest of the parameters given following simulation constraints:

TABLE II
SIMULATION PARAMETERS

Parameter	Value	Parameter	Value
f_{MBS}	2.4 GHz	B_{THz}	10 GHz
f_{mmWave}	73 GHz	$P_{t,\,\mathrm{MBS}}$	30 dB
f_{THz}	0.3 THz	$\alpha_{N,\,\mathrm{mmWave}}$	3.3
B_{MBS}	20 MHz	$\alpha_{L,\,\mathrm{mmWave}}$	2
B_{mmWave}	2 GHz	α_{MBS}	0.5
λ_{UE}	600		

TABLE III
RANGE OF VALUES FOR EACH PARAMETER VARIED IN SIMULATION

Parameter	Simulated Values
$P_{t,\,\mathrm{mmWave}}$	[15, 17.5, 20, 22.5, 25, 27.5, 30, 32.5, 35, 37.5, 40] dBm
$P_{t,\,\mathrm{THz}}$	[15, 17.5, 20, 22.5, 25, 27.5, 30, 32.5, 35, 37.5, 40] dBm
λ_{MBS}	$2 \times 10^{-6}\mathrm{BS}/m^2$
λ_{THz}	[1, 6, 12, 18, 24, 30] $\times\lambda_{\mathrm{MBS}}\mathrm{BS}/m^2$
$\lambda_{\mathrm{mmWave}}$	[1, 4, 8, 12, 26, 20] $\times\lambda_{\mathrm{MBS}}\mathrm{BS}/m^2$

$$\max\ \mathbb{P}(R_{u,j}^{effective} > \eta_j) \text{ subject to following constraints:}$$

$$\text{C1: } \kappa = 50\,\mathbf{kBits/J}$$
$$\text{C2: } \sum_{j=1}^{3} \lambda_j P_{t,j} < P_{total}$$
$$\text{C3: } P_{t,j} > 0$$
$$\text{C4: } \lambda_{MBS} > 0$$
$$\text{C5: } \lambda_{mmWave} > 0$$
$$\text{C6: } \lambda_{THz} > 0$$

The optimization is carried out by calculating the values of THz and mmWave BS densities given the fixed values of parameters then simulating the system at the calculated values.

IV. PERFORMANCE EVALUATION

To evaluate the HetNet framework in different building densities we perform Monte Carlo simulations. The simulation incorporates N users which are spread randomly in the total area of each location mentioned in Table I. Each simulation is repeated over 4 sets of optimization parameters namely small BS transmit power of mmWave and THz, i.e $P_{t,\,\mathrm{mmWave}}$ and $P_{t,\,\mathrm{THz}}$ as well as the densities of BSs in mmWave and THz tier i.e $\lambda_{\mathrm{mmWave}}$ and λ_{THz}. The arrays of variable parameters are shown in Table III. Other parameters such as channel frequencies for each tier, density of the users and path loss exponents are kept constant. The bandwidth for each tier is represented as $\mathrm{B}_{\mathrm{MBS}}$, $\mathrm{B}_{\mathrm{mmWave}}$ and $\mathrm{B}_{\mathrm{THz}}$ for sub 6-GHz, mmWave and THz operation, respectively. A detailed description of all the constant simulation parameters is listed in Table II.

Fig. 4 shows the parameters for peak power efficiency at 6 different building densities under consideration obtained by our simulations. The results reveal that with increasing building density the required mmWave and THz BS densities for peak power efficiency increase initially till the building density of London, i.e. , 34.86%. After this, the required mmWave and THz BS densities start to drop, which shows that in densely populated areas B5G networks are not as effective as in rural or semi-urban zones.

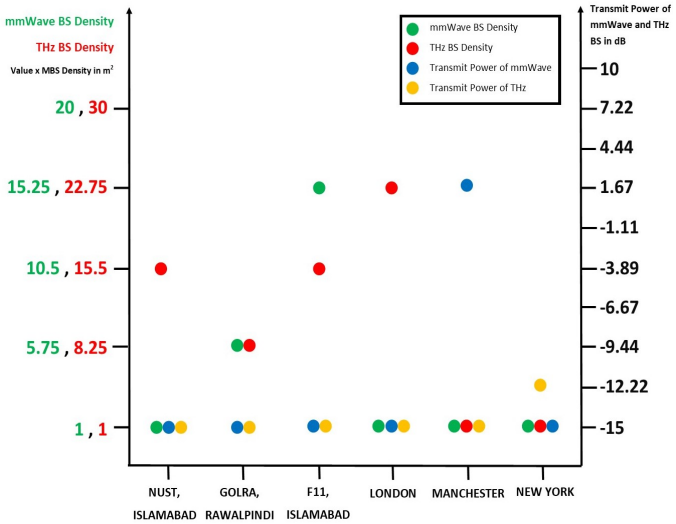

Fig. 4. System parameters for peak power efficiency at 6 different locations. The left vertical axis shows the mmWave and THz BS densities as a multiple of MBS density where $\lambda_{\mathrm{MBS}} = 2 \times 10^{-6}\mathrm{BS}/m^2$. The right vertical axis shows the transmit powers of mmWave and THz in dB while the horizontal axis gives the locations.

Furthermore, for peak power efficiency the system prefers dense mmWave and THz BS deployments with minimum transmission powers in comparison to sparse mmWave and THz BS deployments with higher transmission powers. This is supported by the results of Fig. 5, which show that with increasing THz BS transmit power, while keeping all other parameters constant, the SINR coverage for higher density of THz BS drops. This drop in SINR coverage can be a result of increased interference from adjacent THz BSs due to higher transmission powers.

Fig. 6 illustrates the effective data rate coverage probability against data rate threshold η at two different system settings for each location: minimum system settings are kept at $\lambda_{\mathrm{mmWave}}$ and $\lambda_{\mathrm{THz}} = 2 \times 10^{-6}\mathrm{BS}/m^2$, $P_{t,\,\mathrm{mmWave}}$ and $P_{t,\,\mathrm{THz}} = 15$ dBm while for maximum settings $\lambda_{\mathrm{mmWave}} = 20 \times 10^{-6}\mathrm{BS}/m^2$ and $\lambda_{\mathrm{THz}} = 30 \times 10^{-6}\mathrm{BS}/m^2$, $P_{t,\,\mathrm{mmWave}}$ and $P_{t,\,\mathrm{THz}} = 40$ dBm. There is a stark difference between the deviation in effective data rate coverage of maximum and minimum settings in NUST (5.03 % building area) and New York (51.3 % building area). NUST has considerably lower NLoS links, consequently, increasing THz BS density increases data rate coverage probability more as compared to denser locations.

Similarly, Fig. 7 illustrates the effective rate coverage probability for NUST Campus at the set of simulation parameters given in Table IV, we get the values of mmWave and THz BS densities according to the optimization problem presented in the previous section. Each graph shows the coverage probability at different ratio of $\frac{\lambda_{\mathrm{THz}}}{\lambda_{\mathrm{mmWave}}}$. The results indicate that

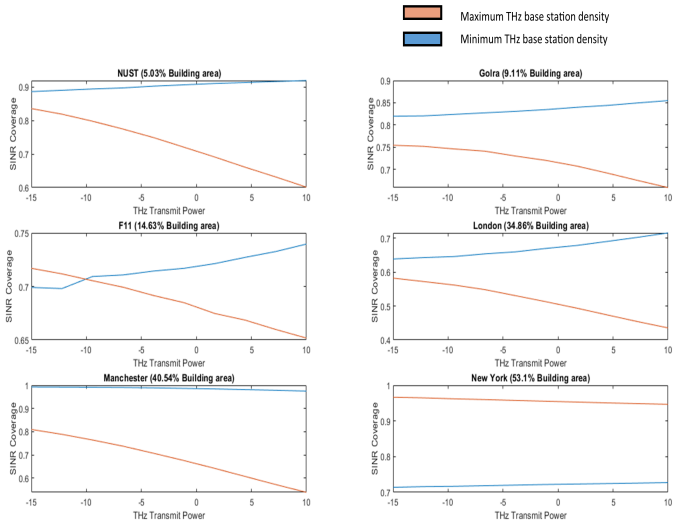

Fig. 5. SINR coverage versus varying THz transmit power for 6 different locations at minimum and maximum λ_{THz} i.e. $2 \times 10^{-6}\mathrm{BS}/m^2$ and $40 \times 10^{-6}\mathrm{BS}/m^2$, with $\lambda_{\mathrm{mmWave}}$ and $P_{t,\,\mathrm{mmWave}}$ kept constant at peak power efficiency from Fig. 4 for each location.

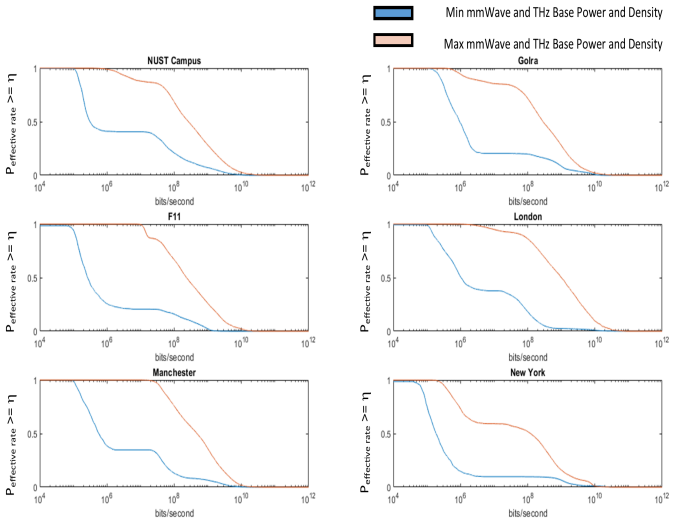

Fig. 6. $P_{effective\,rate}(\eta)$ versus varying data rate threshold η for 6 different locations at minimum and maximum $P_{t,\,THz}$ and $P_{t,\,mmWave}$.

increasing THz BS densities with respect to the mmWave BS density the system experiences elevated data rates however, the coverage probability begins to drop more quickly. This could be attributed to more users being offloaded to THz but experiencing lower stability due to the higher penetration losses at the THz frequencies.

V. Conclusion and Future Work

In this paper, we investigated the coverage and power efficiency characteristics of a 3-tier HetNet comprising sub-6 GHz, mmWave and THz frequencies for different building densities. The preceding analysis indicates that with increasing building density, the THz/mmWave deployment complexity

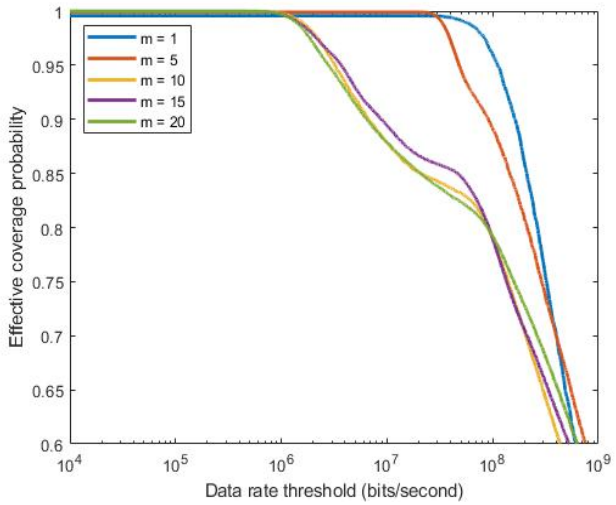

Fig. 7. Effective rate coverage probability versus Data rate threshold for different values of m while keeping $P_{t,\,\mathrm{MBS}}$, $P_{t,\,\mathrm{THz}}$, $P_{t,\,\mathrm{mmWave}}$, and λ_{MBS} constant at 40 dBm, 23 dBm, 23 dBm, and $2 \times 10^{-6}\mathrm{BS}/m^2$, respectively

required to maintain a given QoS also increases. Thus, our results support the intuitive observation that using traditional transmission methods, B5G networks may only be effective in low-obstruction, open areas. Furthermore, peak power efficiency require denser mmWave and THz BS deployement in less building densities like NUST as compared to Manchester and New York. Our results conclude that if we keep all the simulation parameters constant except the THz transmit power for maximum THz base station density, the SINR coverage of the system decreases drastically for increasing THz transmit power. Due to the random nature of wireless channels, a generalized model for the deployment of B5G systems may not be devised without the use of statistical analysis or artificial intelligence techniques. In the future, AI may offer a holistic approach for system analysis which will eliminate the need to know exact blockage environments and reduce computational complexity.

Acknowledgment

The work of H. Jung was supported by the Ministry of Science and ICT, Korea under the Information Technology Research Center support program (IITP-2021-0-02046).

References

[1] T. Alam, "A reliable communication framework and its use in internet of things (IoT)," *International Journal of Scientific Research in Computer Science, Engineering and Information Technology*, vol. 3(5), pp. 450–456, 2018.

[2] Y. Lu and X. Zheng, "6G: A survey on technologies, scenarios, challenges, and the related issues," *Journal of Industrial Information Integration*, p. 100158, Jul. 20.

[3] Y. Niu, Y. Li, D. Jin, L. Su, and A. V. Vasilakos, "A survey of millimeter wave communications (mmWave) for 5G: opportunities and challenges," *Wireless Networks*, vol. 21, no. 8, pp. 2657–2676, Nov. 20.

[4] I. F. Akyildiz, C. Han, and S. Nie, "Combating the distance problem in the millimeter wave and terahertz frequency bands," *IEEE Communications Magazine*, vol. 56, no. 6, pp. 102–108, Jun. 2018.

[5] I. F. Akyildiz, J. M. Jornet, C. Han, "Terahertz band: Next frontier for wireless communications" *Physical Communication*, Volume 12, Pages 16-32, 2014.

[6] A. Umer, S. A. Hassan, H. Pervaiz, L. Musavian, Q. Ni, and M. A. Imran, "Secrecy spectrum and energy efficiency analysis in massive mimoenabled multi-tier hybrid hetnets," *IEEE Transactions on Green Communications and Networking*, 2019.

[7] J. M. Jornet and I. F. Akyildiz, "Channel modeling and capacity analysis for electromagnetic wireless nanonetworks in the terahertz band," *IEEE Transactions on Wireless Communications*, vol. 10, no. 10, pp. 3211–3221, 2011.

[8] M. S. Omar, M. A. Anjum, S. A. Hassan, H. Pervaiz and Q. Niv, "Performance analysis of hybrid 5G cellular networks exploiting mmWave capabilities in suburban areas," *IEEE International Conference on Communications (ICC)*, pp. 1-6, 2016.

[9] C. Lin and G. Y. Li, "Indoor terahertz communications: How many antenna arrays are needed?" *IEEE Transactions on Wireless Communications*, vol. 14, no. 6, pp. 3097–3107, 2015.

[10] L. S. Rothman, "The hitran 2008 molecular spectroscopic database," *Journal of Quantitative Spectroscopy and Radiative Transfer*, vol. 110, no. 9-10, pp. 533–572, 2009.

[11] A. A. Raja, M. A. Jamshed, H. Pervaiz and S. A. Hassan, "Performance Analysis of UAV-assisted Backhaul Solutions in THz enabled Hybrid Heterogeneous Network," *IEEE INFOCOM 2020 - IEEE Conference on Computer Communications Workshops (INFOCOM WKSHPS)*, pp. 628-633, 2020 (NUST), Islamabad,